Original Article | Musculoskeletal Imaging

eISSN 2005-8330
https://doi.org/10.3348/kjr.2020.0548
Korean J Radiol 2021;22(8):1341-1351

Korean Journal of Radiology
KJR

Comparison of the Quality of Various Polychromatic and Monochromatic Dual-Energy CT Images with or without a Metal Artifact Reduction Algorithm to Evaluate Total Knee Arthroplasty

Hye Jung Choo, Sun Joo Lee, Dong Wook Kim, Yoo Jin Lee, Jin Wook Baek, Ji-yeon Han, Young Jin Heo

All authors: Department of Radiology, Inje University Busan Paik Hospital, Busan, Korea

Objective: To compare the quality of various polychromatic and monochromatic images with or without using an iterative metal artifact reduction algorithm (iMAR) obtained from a dual-energy computed tomography (CT) to evaluate total knee arthroplasty.

Materials and Methods: We included 58 patients (28 male and 30 female; mean age [range], 71.4 [61–83] years) who underwent 74 knee examinations after total knee arthroplasty using dual-energy CT. CT image sets consisted of polychromatic image sets that linearly blended 80 kVp and tin-filtered 140 kVp using weighting factors of 0.4, 0, and -0.3, and monochromatic images at 130, 150, 170, and 190 keV. These image sets were obtained with and without applying iMAR, creating a total of 14 image sets. Two readers qualitatively ranked the image quality (1 [lowest quality] through 14 [highest quality]). Volumes of high- and low-density artifacts and contrast-to-noise ratios (CNRs) between the bone and fat tissue were quantitatively measured in a subset of 25 knees unaffected by metal artifacts.

Results: iMAR-applied, polychromatic images using weighting factors of -0.3 and 0.0 ($P_{-0.3i}$ and $P_{0.0i}$, respectively) showed the highest image-quality rank scores (median of 14 for both by one reader and 13 and 14, respectively, by the other reader; $p < 0.001$). All iMAR-applied image series showed higher rank scores than the iMAR-unapplied ones. The smallest volumes of low-density artifacts were found in $P_{-0.3i}$, $P_{0.0i}$, and iMAR-applied monochromatic images at 130 keV. The smallest volumes of high-density artifacts were noted in $P_{-0.3i}$. The CNRs were best in polychromatic images using a weighting factor of 0.4 with or without iMAR application, followed by polychromatic images using a weighting factor of 0.0 with or without iMAR application.

Conclusion: Polychromatic images combined with iMAR application, $P_{-0.3i}$ and $P_{0.0i}$, provided better image qualities and substantial metal artifact reduction compared with other image sets.

Keywords: *Dual-energy CT; Total knee arthroplasty; Prosthesis; Metal artifact reduction; Virtual monochromatic imaging*

INTRODUCTION

Accurate interpretation of computed tomography (CT) images with metallic implants is challenging because of metal-induced artifacts. These usually present as bright and dark streaks caused by multiple mechanisms such as photon starvation, beam hardening, scattering, partial volume effects, and edge effects [1-3]. The severity of the impact of metal artifacts on CT is dependent on the size and atomic number of the metallic implant. For instance, smaller implants show fewer metal-induced artifacts and implants with higher atomic numbers, such as cobalt (atomic number 27) and chromium (atomic number 24), show more metal-induced artifacts [2]. Because orthopedic metallic implants are usually larger and made of materials with higher atomic

Received: April 29, 2020 **Revised:** February 1, 2021
Accepted: February 5, 2021
Corresponding author: Hye Jung Choo, MD, PhD, Department of Radiology, Inje University Pusan Paik Hospital, 75 Bokji-ro, Busanjin-gu, Busan 47392, Korea.
• E-mail: hyejungchoo@gmail.com
This is an Open Access article distributed under the terms of the Creative Commons Attribution Non-Commercial License (https://creativecommons.org/licenses/by-nc/4.0) which permits unrestricted non-commercial use, distribution, and reproduction in any medium, provided the original work is properly cited.

Copyright © 2021 The Korean Society of Radiology

numbers, metal-induced artifacts are very troublesome in the field of musculoskeletal radiology.

Many strategies have been developed to reduce these metal artifacts. These strategies can be categorized into two approaches [2,4]. One is the use of high-energy reconstruction of virtual monochromatic images created with dual-energy CT (DECT). High-energy photons in high-energetic virtual monochromatic images can reduce beam hardening artifacts without increasing the patient's radiation exposure; however, this leads to a decreased tissue contrast [5-7]. The other approach incorporates the use of a metal artifact reduction algorithm (MAR), a sinogram in-painting technique, which identifies corrupted projection data caused by the presence of metals and subsequently replaces them with approximated or interpolated data. Metal artifact reduction lowers the effects of beam hardening and photon starvation [4]. Currently, several vendors offer their own versions of MAR: iterative MAR (iMAR, Siemens Healthineers), MAR for orthopedic implants (O-MAR, Philips Healthcare), single-energy MAR (SEMAR, Canon Medical Systems), and smart MAR (SmartMAR, GE Healthcare) [5-8]. A few recent studies have dealt with the combination of virtual monochromatic images and MAR [9-13]. Bongers et al. [9] and Long et al. [12] showed that combining these two methods showed the best metal artifact reduction. Conversely, Khodarahmi et al. [10] reported that this combination did not improve image quality over exclusive MAR use for polychromatic data.

DECT provides linearly blended polychromatic images to fuse high- and low-energy images with different weighting factors. For example, a weighting factor of 0.3 means that 30% of the image information is derived from the low-energy image and 70% from the high-energy image. As the weighting factor increases, the image appears to be a more low energy image. In DECT with tube voltages of 80 kVp and 140 kVp, a polychromatic image with a weighting factor of 0.3 corresponds approximately to a 120-kVp image [14-16]. Therefore, blended polychromatic images with lower weighting factors could simulate higher-kVp images. Combined with MAR, this strategy could be a good method for metal artifact reduction.

Therefore, our study attempted to compare the quality of various polychromatic and monochromatic images with or without applying an iterative metal artifact reduction algorithm (iMAR) obtained from a DECT to evaluate total knee arthroplasty.

MATERIALS AND METHODS

This retrospective exploratory study was approved by the Institutional Review Board of Inje University Busan Paik Hospital, and the need for informed consent was waived (IRB No. 19-0234).

Study Population

We included 58 patients who underwent DECT of the knees after total knee arthroplasty between January 2019 and January 2020. Of these patients, 28 were male and 30 were female (mean age, 71.4 years; age range, 61–83 years). Forty-two patients underwent unilateral knee arthroplasty, and the rest underwent bilateral knee arthroplasty. Among all 74 cases of total knee arthroplasty, 67 were performed in our institution and the others elsewhere.

Image Acquisition

All CT images in this study were obtained using a dual-source DECT scanner (Somatom Drive, Siemens Healthineers). The scanning parameters were a tube voltage of 80 kVp and a tin-filter (Sn) of 140 kVp; an effective tube current time of 200 mAs and 100 mAs for the low- and high-kVp settings, respectively; an automatic tube current modulation with the quality reference tube current-time product of 192 mAs; a slice acquisition of 32 x 0.6 mm; a pitch of 0.7; a rotation time of 1 second; and a volume CT dose index of 7.79 mGy.

Image Reconstruction

Six polychromatic images and eight monochromatic images were reconstructed. During the reconstruction of the polychromatic images, low- and high-kVp sources were linearly blended with three weighting factors of 0.4, 0.0, and -0.3. Polychromatic images with weighting factors of 0.4, 0.0, and -0.3 were generated by mixing 40% of 80-kVp images and 60% of Sn 140-kVp images, 0% of 80-kVp images and 100% of Sn 140-kVp images, and -30% of 80-kVp images and 130% of Sn 140-kVp images, respectively. A polychromatic image with a weighting factor of 0.4 was equivalent to a 120-kVp image according to the vendor's reference. Because a DECT with 80 kVp and Sn 140 kVp (not 80 kVp and 140 kVp) was utilized in this study, the weighting factor corresponding to 120 kVp was higher than 0.3. Monochromatic images were obtained at 130 keV, 150 keV, 170 keV, and 190 keV. Using the guidelines above, with or without iMAR, six polychromatic images

https://doi.org/10.3348/kjr.2020.0548

Korean Journal of Radiology
KJR

and eight monochromatic images were generated (iMAR-applied, polychromatic images with weighting factors of 0.4, 0.0, and -0.3 [$P_{0.4i}$, $P_{0.0i}$, $P_{-0.3i}$, respectively] and iMAR-unapplied, polychromatic images with weighting factors of 0.4, 0.0, and -0.3 [$P_{0.4}$, $P_{0.0}$, and $P_{-0.3}$, respectively], iMAR-applied, monochromatic images at 130 keV, 150 keV, 170 keV, and 190 keV [M_{130i}, M_{150i}, M_{170i}, and M_{190i}, respectively], and iMAR-unapplied monochromatic images at 130, 150, 170, and 190 keV [M_{130}, M_{150}, M_{170}, and M_{190}, respectively]) (Table 1). The selected option for iMAR was "extremity implant" because we considered this to be the superior choice in patients with knee arthroplasty. All images were reconstructed in the axial plane with a slice thickness of 3 mm, soft tissue kernel (I40), and advanced modeled iterative reconstruction (ADMIRE, Siemens Healthineers) at a strength of 3. Immediately after image acquisition, polychromatic image series were reconstructed on a regular workstation by the technicians. At a later time, monochromatic image series (or polychromatic images when they were incompletely provided) were reconstructed by a radiologist using dedicated softwares (Mono+, SyngoVia, version VB 30A_HF02, Siemens Healthineers).

Image Analysis

Qualitative Image Quality

Two radiologists (readers A and B), each with more than ten years of experience in musculoskeletal radiology, independently ranked the overall image quality of the datasets of all participants. They considered metal artifact reduction and visibility of the bone–implant interface and bone and soft tissue details in side-by-side comparisons. Rank scores from 1 to 14 were given because there were 14 image sets, with 14 indicating the best image quality and 1 indicating the worst. Tied ranks were permitted: for example, if there were two image sets assigned a score of 14, the next best image set (i.e., the third best image quality ranking) was given a score of 12. While scoring the images, the 14-image series from each dataset were randomly displayed in the picture archiving and communications system (PACS) software after removing the digital imaging and communication in medicine (DICOM) header information and annotations to blind the readers to patient and image series information. All datasets were shown with a window width of 600 Hounsfield unit (HU) and a window level of 150 HU. In cases of bilateral knee arthroplasties, the right knee was assessed.

Quantitative Image Quality

Reader A performed all measurements and calculations in a subset of 25 knees of 20 patients (6 male, 14 female; mean age, 71.3 years; age range, 61–83 years; unilateral knee arthroplasty in 15 patients, bilateral knee arthroplasty in 5 patients) of the 58 participants because the source CT data in the other patients were inadequate for these quantitative analyses.

The volumes of the low- and high-density artifacts were separately measured because metallic artifacts appear

Table 1. CT Image Series

iMAR	Monochromatic vs. Polychromatic	Photon Energy	Image Series Description
Unapplied	Polychromatic	Blending of 80 and 140 kVp	iMAR-unapplied, polychromatic image with a weighting factor of 0.4 ($P_{0.4}$)
		Blending of 80 and 140 kVp	iMAR-unapplied, polychromatic image with a weighting factor of 0.0 ($P_{0.0}$)
		Blending of 80 and 140 kVp	iMAR-unapplied, polychromatic image with a weighting factor of -0.3 ($P_{-0.3}$)
	Monochromatic	130 keV	iMAR-unapplied, monochromatic image at 130 keV (M_{130})
		150 keV	iMAR-unapplied, monochromatic image at 150 keV (M_{150})
		170 keV	iMAR-unapplied, monochromatic image at 170 keV (M_{170})
		190 keV	iMAR-unapplied, monochromatic image at 190 keV (M_{190})
Applied	Polychromatic	Blending of 80 and 140 kVp	iMAR-applied, polychromatic image with a weighting factor of 0.4 ($P_{0.4i}$)
		Blending of 80 and 140 kVp	iMAR-applied, polychromatic image with a weighting factor of 0.0 ($P_{0.0i}$)
		Blending of 80 and 140 kVp	iMAR-applied, polychromatic image with a weighting factor of -0.3 ($P_{-0.3i}$)
	Monochromatic	130 keV	iMAR-applied, monochromatic image at 130 keV (M_{130i})
		150 keV	iMAR-applied, monochromatic image at 150 keV (M_{150i})
		170 keV	iMAR-applied, monochromatic image at 170 keV (M_{170i})
		190 keV	iMAR-applied, monochromatic image at 190 keV (M_{190i})

iMAR = iterative metal artifact reduction algorithm

https://doi.org/10.3348/kjr.2020.0548

as streaks and dark/bright regions. The upper and lower boundaries of the volume of interest (VOI) were the upper end of the femoral component of the implant and the proximal aspect of the proximal tibiofibular joint, respectively, which were the same across the image series in each dataset. The background was excluded from the VOI. A maximal threshold of -400 HU in the VOI was used to measure low-density artifacts, and a minimal threshold of 800 HU was used for high-density artifacts [10]. High-density artifact quantifications include the volume of metallic implants. These measurements were performed with a SyngoVia workstation (Siemens Healthineers) (Fig. 1).

To evaluate the effects of iMAR and mono- or polychromatic images on CT attenuation, background noise, contrast-to-noise ratio (CNR), CT attenuation numbers of the bone and fat, and background noise on the image slices not affected by the metal artifacts were measured on the PACS. The location and size of the region of interest (ROI) for measurements were the same across the series in each dataset. Because cancellous bone may be affected by the status of bone marrow and bone mass, the cortical bone of the femoral shaft was selected for the bone ROI. Fat tissue devoid of vessels was used to determine the fat ROI, and the image corners were used to determine the background ROI. The ROI size was approximately 3 mm^2; this was adaptively manipulated to avoid inclusion of unrepresentative tissue. The standard deviations of CT attenuation numbers in the background ROIs were used as the background noise. Each measurement was performed three times, and averages were analyzed. The CNR was then calculated by dividing the difference in the CT attenuation numbers between bone and fat by the background noise.

Statistical Analysis

Using the Shapiro–Wilk test, we found that the continuous variables were not normally distributed (volume of the artifacts, CT attenuation number, noise, and CNR). Thus, the continuous variables and ordinal variables (rank scores of image quality) among the 14-image series were compared using the Friedman's test followed by a multiple pairwise comparison with the Conover's test. During the multiple pairwise comparisons, *p* values were adjusted using the Bonferroni method. The inter-reader agreement on the rank scores of image quality was analyzed using the weighted κ test. The degree of agreement was categorized as follows: < 0, poor; 0–0.20, slight agreement; 0.21–0.40, fair agreement; 0.41–0.60, moderate agreement; 0.61–0.80, substantial agreement; and 0.81–1, almost perfect

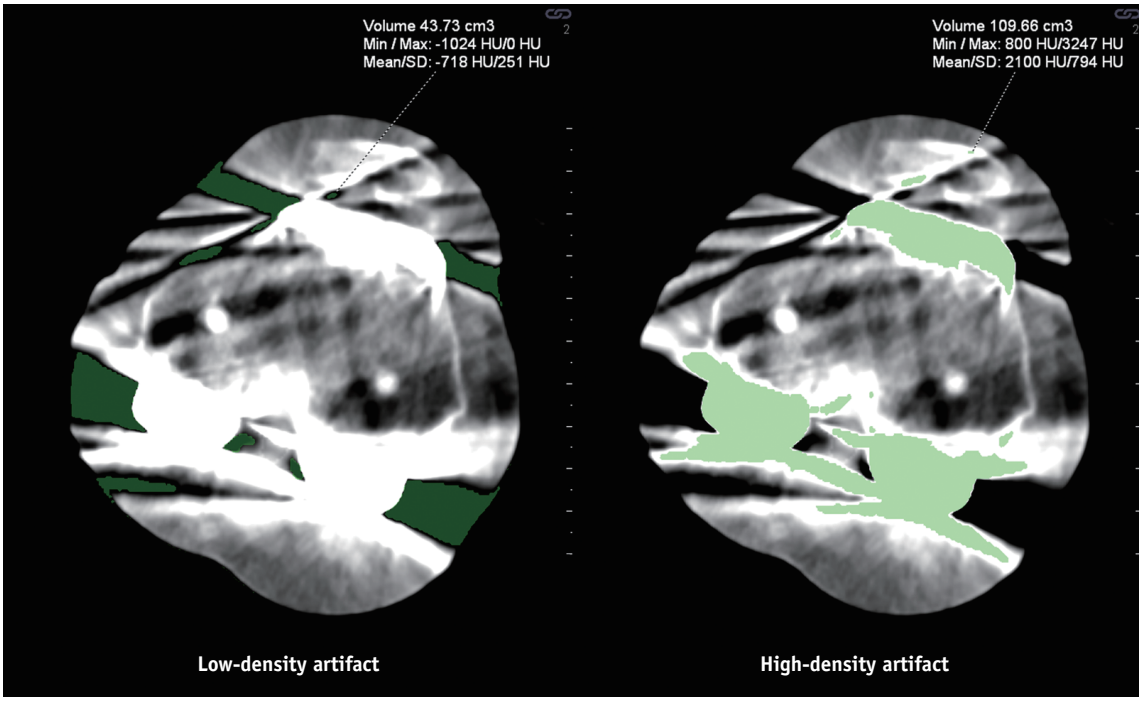

Fig. 1. Measurement of volumes of low- and high-density artifacts. Post-processed color-coded 130-keV monochromatic images without an iterative metal artifact reduction algorithm show dark green areas indicating low-density artifacts with a maximal threshold of -400 HU and light green areas indicating high-density artifacts with a minimal threshold of 800 HU. HU = Hounsfield unit, Max = maximum, Min = minimum, SD = standard deviation

https://doi.org/10.3348/kjr.2020.0548

Korean Journal of Radiology
KJR

agreement [17]. All statistical analyses were performed using SPSS (version 24, IBM Corp.) and Rex (version 3.0.3, RexSoft Inc.). A two-sided *p* value of < 0.001 was considered statistically significant.

RESULTS

Qualitative Image Quality

Among the 14-image series by the two readers, $P_{0.0i}$ and $P_{-0.3i}$ had the best rank scores for image quality (Table 2). Along with significant metal artifact reduction, $P_{-0.3i}$ showed good bone–metal interface, and $P_{0.0i}$ showed good tissue contrast (Fig. 2). M_{130i} showed the second best rank scores, followed by M_{150i} and M_{170i}. All image series combined with the iMAR application showed significantly higher rank scores than those without. Among the iMAR-unapplied image series, $P_{-0.3}$ showed the best rank scores. The inter-reader agreement was substantial ($\kappa = 0.802$).

Low- and High-Density Artifacts

The volumes of the low- and high-density artifacts were significantly different among the 14-image series ($p <$ 0.001). $P_{0.0i}$, $P_{-0.3i}$, and M_{130i} showed the lowest volumes of low-density artifacts (Figs. 2, 3A). The volumes of the high-density artifacts were lowest in $P_{-0.3i}$, followed by $P_{0.0i}$ and M_{130i}. $P_{0.4}$ had the largest volumes of low- and high-density artifacts (Figs. 2, 3B). All iMAR-applied image series, except $P_{0.4i}$, had fewer low- and high-density artifacts than the iMAR-unapplied series. The monochromatic image series showed an increasing trend of low-density artifacts with higher photon energies and a decreasing trend of high-density artifacts with higher photon energies.

CT Attenuation, CNR, and Noise

CT attenuation numbers of tissues, background noise, and CNRs significantly differed among the 14-image series ($p <$ 0.001) (Figs. 2, 4). The CT attenuation numbers of bone tended to decrease with lower weighting factors in polychromatic images and higher photon energies in monochromatic images (Fig. 4A), whereas those of fat tended to increase with lower weighting factors and higher photon energies (Fig. 4B). $P_{0.4}$ and $P_{0.4i}$ showed the highest CT attenuation of bone and the lowest CT attenuation of fat, whereas $P_{-0.3}$ and $P_{-0.3i}$ showed the lowest attenuation of bone and the highest attenuation of fat. Consequently, the CNRs were the best in $P_{0.4}$ and $P_{0.4i}$, and worst in $P_{-0.3}$ and $P_{-0.3i}$ (Fig. 4C). The next best CNRs were found in $P_{0.0}$, $P_{0.0i}$, and M_{130}. The combination of iMAR did not influence the CT attenuation numbers of fat and slightly decreased those of bone. The background noise was significantly higher in $P_{-0.3}$ and $P_{-0.3i}$ (Fig. 4D). The application of iMAR mildly increased the background noise.

DISCUSSION

In this study, $P_{-0.3i}$ and $P_{0.0i}$ showed the best qualitative image quality in patients who underwent total knee arthroplasty. Quantitatively, $P_{-0.3i}$ had the lowest volumes

Table 2. Qualitative Image Quality Analysis

	Reader A		Reader B	
	Ranks Score*	Image Sets Showing Statistical Difference†	Ranks Score*	Image Sets Showing Statistical Difference†
$P_{0.4}$	1 (1–1)	All	1 (1–1)	All
$P_{0.0}$	2 (2–6)	All	2 (2–2.3)	All
$P_{-0.3}$	7 (3–7)	All except M_{170}, M_{190}	7 (6–7)	All except M_{170}, M_{190}
M_{130}	6 (5–7)	All except M_{150}, M_{170}, M_{190}	6 (4.3–6)	All except M_{150}, M_{170}, M_{190}
M_{150}	6 (5–7)	All except M_{130} M_{170}, M_{190}	6 (5–5.8)	All except M_{130}, M_{170}, M_{190}
M_{170}	6 (5–7)	All except M_{130}, M_{150}, M_{190}	6 (5.3–6)	All except M_{130}, M_{150}, M_{190}
M_{190}	6 (5–7)	All except M_{130}, M_{150}, M_{170}	6 (5–6)	All except M_{130}, M_{150}, M_{170}
$P_{0.4i}$	8 (8–8)	All	8 (8–8)	All
$P_{0.0i}$	14 (13–14)	All except $P_{-0.3i}$	14 (14–14)	All except $P_{-0.3i}$
$P_{-0.3i}$	14 (13–14)	All except $P_{0.0i}$	13 (13–14)	All except $P_{0.0i}$
M_{130i}	12 (12–12)	All	12 (12–12)	All
M_{150i}	11 (11–12)	All except M_{170i}	11 (11–12)	All except M_{170i}
M_{170i}	11 (10–11)	All except M_{150i}, M_{190i}	11 (11–12)	All except M_{150i}, M_{190i}
M_{190i}	11 (10–11)	All except M_{170i}	11 (9–11)	All except M_{170i}

*Data are median (interquartile range), †Data are from pairwise comparisons between the image sets. *P* < 0.001 (i.e., Bonferroni-adjustment) were only included.

https://doi.org/10.3348/kjr.2020.0548

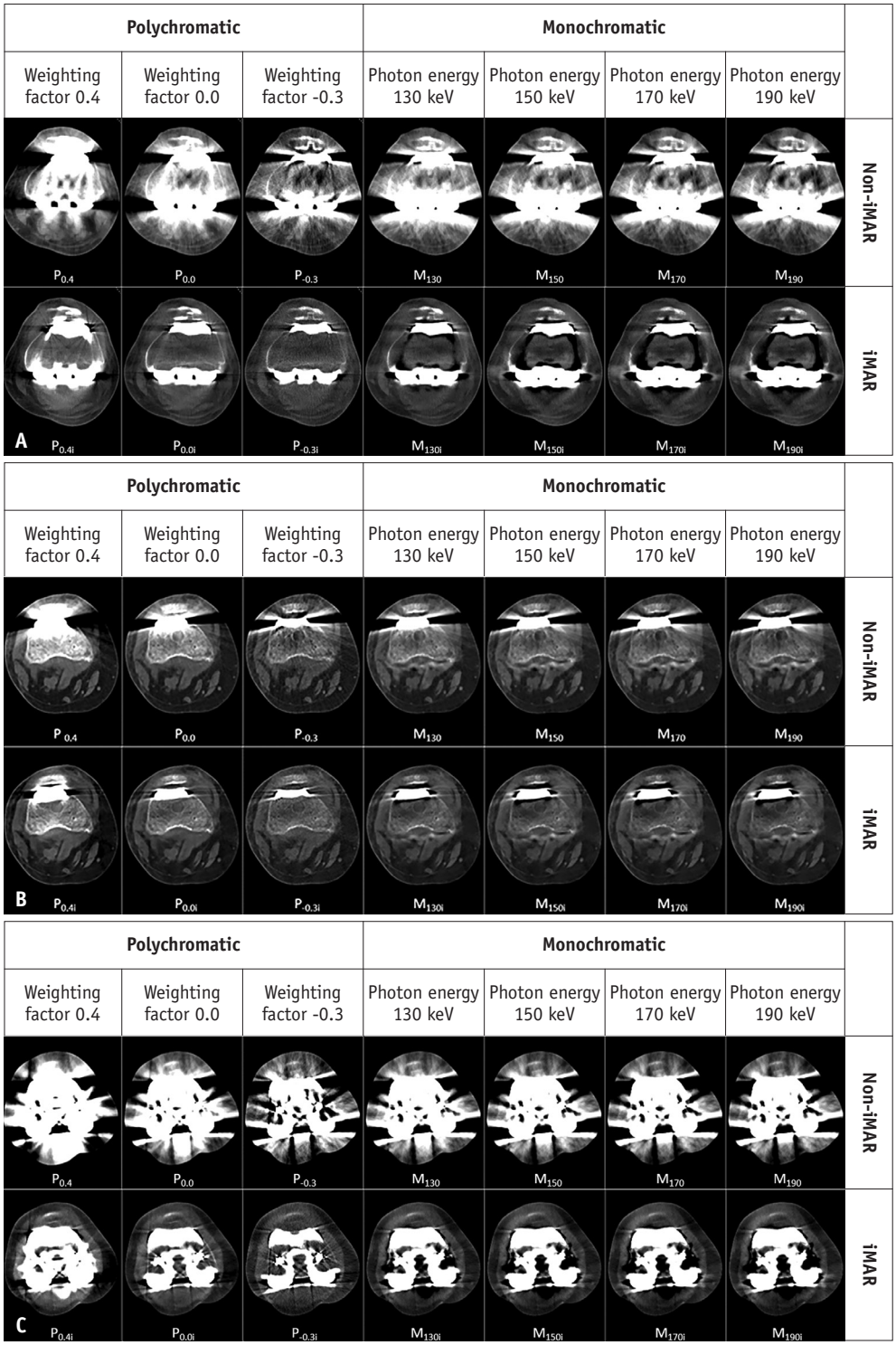

Fig. 2. CT image series in a 68-year-old male with right knee arthroplasty (A), in a 70-year-female with right knee arthroplasty (B), and in a 68-year-old female with right knee arthroplasty (C). The iMAR-applied image series (lower row) shows obvious metal artifact reduction, compared with the iMAR-unapplied image series (upper row). The iMAR-applied, polychromatic images with a weighting factor of -0.3 ($P_{-0.3i}$) show the best metal-bone-interface and least low-density and high-density metal artifacts, although they are somewhat coarse and noisy. Monochromatic image series with iMAR application show an increasing trend of low-density artifacts with higher photon energies. The iMAR-applied, polychromatic images with a weighting factor of 0.0 ($P_{0.0i}$) show comparable metal-bone interface with that of iMAR-applied, monochromatic images at 130 KeV (M_{130i}), but less low-density metal artifact and better tissue contrast (higher bone density and lower fat density) than M_{130i}. All the images were displayed with a window width of 600 HU and a window level of 150 HU. HU = Hounsfield unit, iMAR = iterative metal artifact reduction algorithm

https://doi.org/10.3348/kjr.2020.0548

Korean Journal of Radiology
KJR

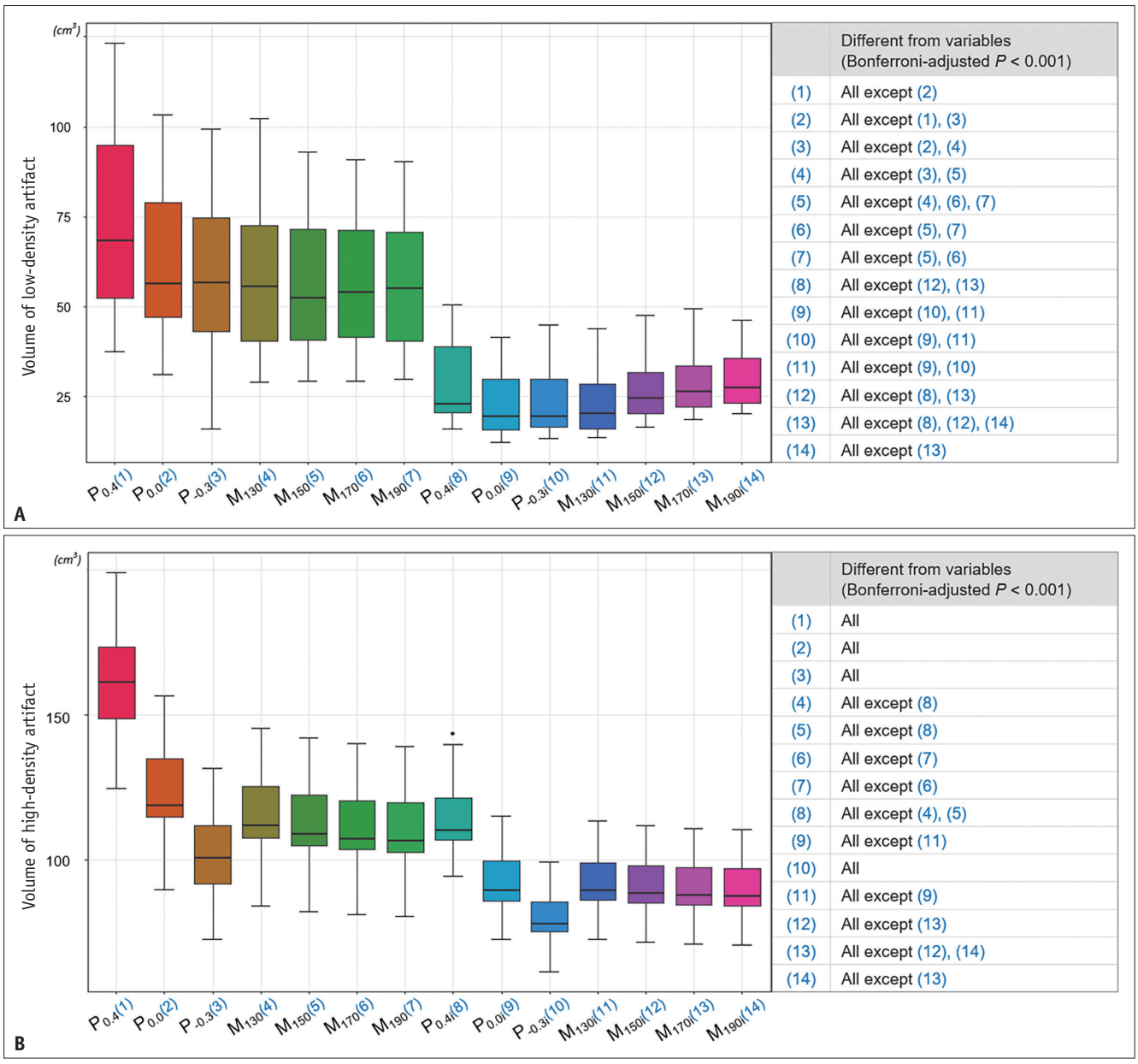

Fig. 3. Box-and-whisker plots of volumes of low-density artifacts (A) and high-density artifacts (B) with corresponding multiple pairwise comparison tests. iMAR-applied, polychromatic images with weighting factors of 0.0 and -0.3 ($P_{0.0i}$ and $P_{-0.3i}$) and iMAR-applied monochromatic images at 130 keV (M_{130i}) show the lowest low-density artifacts. $P_{-0.3i}$ shows the lowest high-density artifacts. As the weighting factors of blended polychromatic images decrease and photon energies of monochromatic images increase, the high-density artifacts show a decreasing tendency and the low-density artifacts show an increasing tendency. iMAR = iterative metal artifact reduction algorithm

of low- and high-density artifacts; however, it showed the worst CNRs and the highest background noise. $P_{0.0i}$ and M_{130i} had the second lowest volumes of low- and high-density artifacts. Between them, CNRs were better in $P_{0.0i}$ than in M_{130i}.

To date, few studies have been evaluated the usefulness of MAR and virtual monochromatic images [9-13]. Most of these studies concluded that the combination yielded optimal artifact reduction, compared to each method alone [9,11-13]. Bongers et al. [9] compared the metal artifact reduction performance of 120-kVp-equivalent mixed polychromatic images and monochromatic images at 130 keV with or without iMAR on hip prostheses and dental implants. They concluded that the combination of iMAR and monochromatic images provided a considerable benefit compared to each method alone. However, a study by Khodarahmi et al. [10] compared the volumes of low- and high-density artifacts among 120-kVp-equivalent

https://doi.org/10.3348/kjr.2020.0548

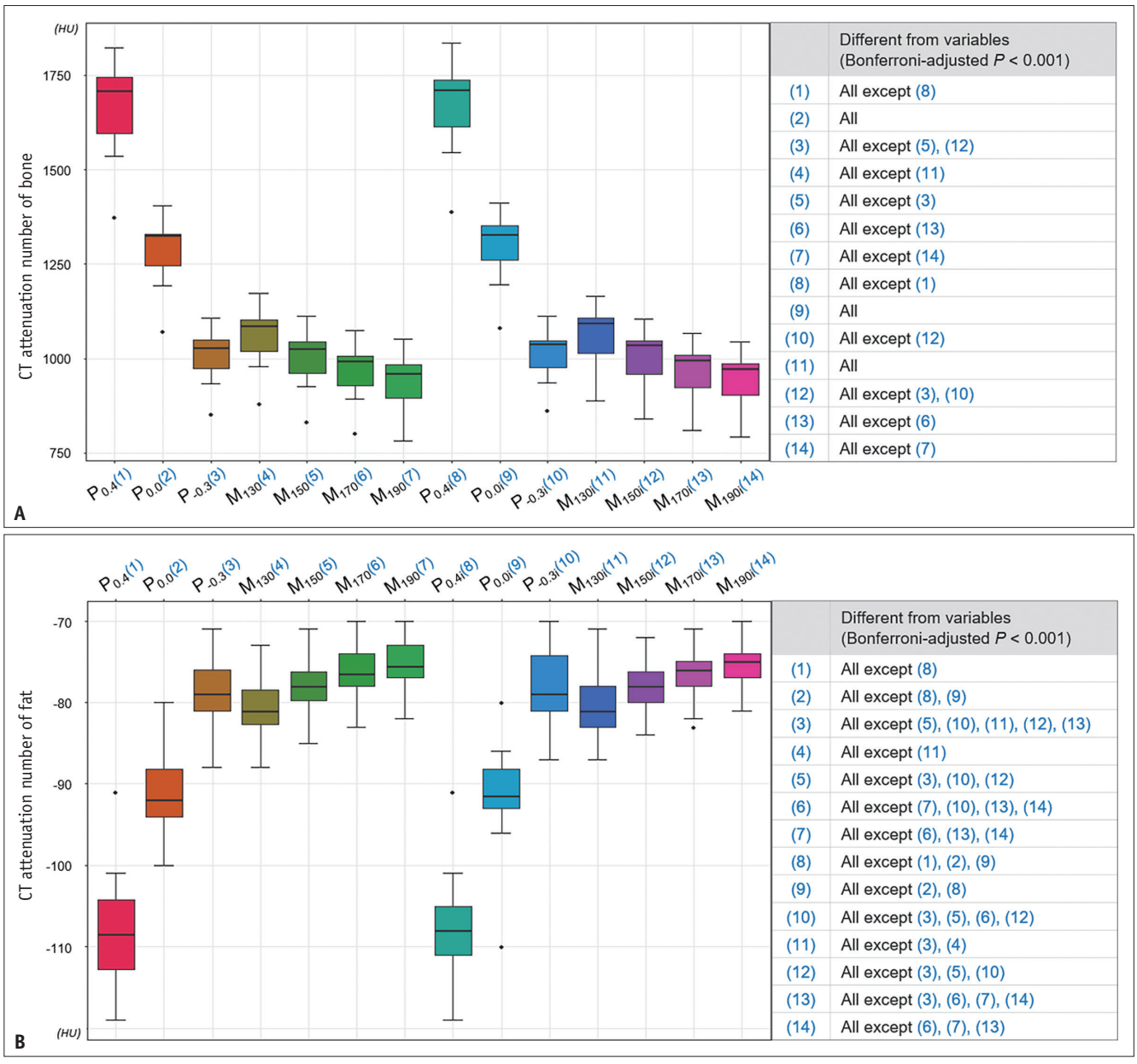

Fig. 4. Box-and-whisker plots of CT attenuation numbers of bone (A) and fat (B), CNRs (C), and background noise (D) with corresponding multiple pairwise comparison tests. As weighting factors decrease and photon energies increase, bone attenuation decreases and fat attenuation increases. Polychromatic images with a weighting factor of -0.3 with and without iterative metal artifact reduction algorithm application ($P_{-0.3i}$, $P_{-0.3}$) show the lowest CNRs and the highest background noise. CNR = contrast-to-noise ratio

polychromatic images and monochromatic images at 150 keV and 190 keV with or without iMAR on ankle arthroplasty and concluded that the combination of iMAR and virtual monochromatic images at higher photon energies did not improve image quality over iMAR-reconstructed mixed polychromatic data alone. They found that the combination at higher energies resulted in mixed effects on metallic artifacts, including decreased high-density artifacts and increased low-density artifacts. Our results partially agree with those of Bongers et al. [9], as iMAR-applied monochromatic images at 130 keV were superior to iMAR-applied 120-kVp-equivalent polychromatic images for metal artifact reduction. Our results also partially agree with those of Khodarahmi et al. [10], as monochromatic images tended to have increased low-density artifacts and decreased high-density artifacts as photon energies increased.

The major strength of our study lies in the novel use of polychromatic images with low weighting factors for metal artifact reduction, rather than routinely used polychromatic images equivalent to 120 kVp. As per our expectations,

https://doi.org/10.3348/kjr.2020.0548

Korean Journal of Radiology
KJR

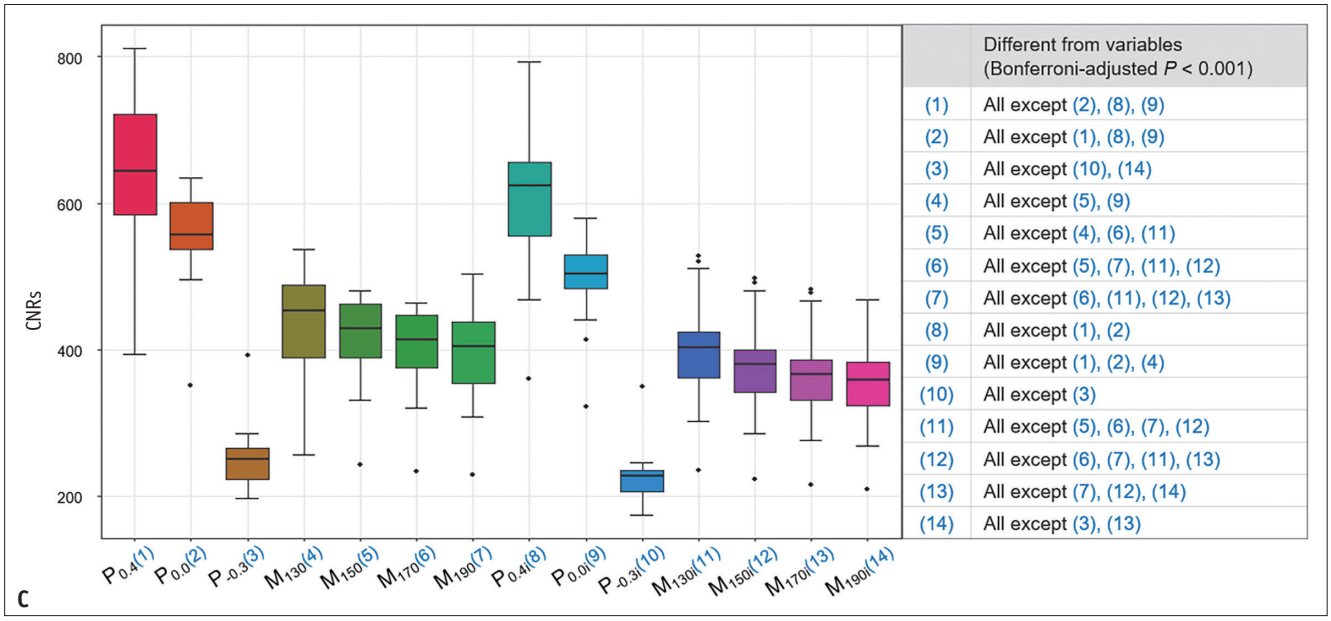

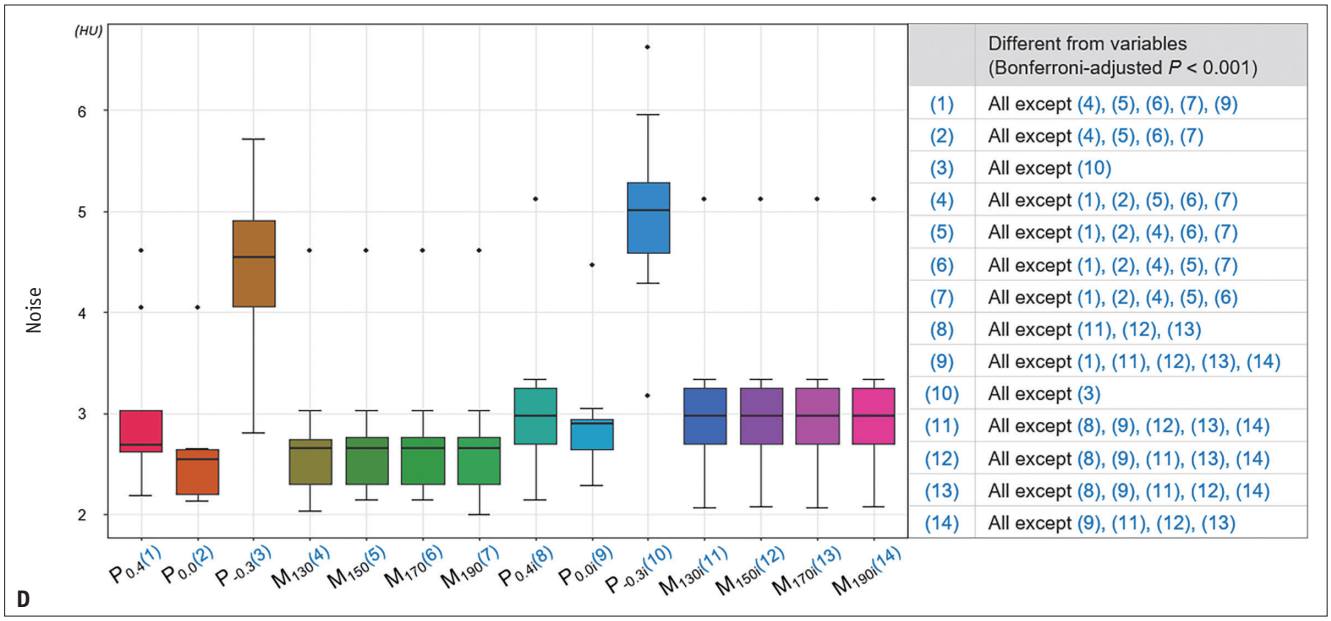

Fig. 4. Box-and-whisker plots of CT attenuation numbers of bone (A) and fat (B), CNRs (C), and background noise (D) with corresponding multiple pairwise comparison tests. As weighting factors decrease and photon energies increase, bone attenuation decreases and fat attenuation increases. Polychromatic images with a weighting factor of -0.3 with and without iterative metal artifact reduction algorithm application ($P_{-0.3i}$, $P_{-0.3}$) show the lowest CNRs and the highest background noise. CNR = contrast-to-noise ratio

blended polychromatic images with low weighting factors of 0.0 and -0.3, presumably corresponding to images with an of Sn 140 kVp and those with a higher kVp, respectively, yielded a better metal artifact reduction and image quality than 120-kVp-equivalent polychromatic images and higher-energy monochromatic images. Another notable point of our study is the use of a tin filter in a high-kVp tube. A tin filter added to a standard aluminum filter increases the mean photon energy without increasing radiation exposure by absorbing low-energy photons [18]. Thus, tin-filtered high-kVp photons can reduce beam hardening and decrease metal artifacts. A recent study using photon-counting CT demonstrated that high-energy threshold images acquired with tin filtration yielded a substantial decrease in metal artifacts [19]. The fact that $P_{0.0i}$, theoretically equivalent to Sn 140 kVp, showed the best rank may be firmly related to the use of tin-filtered high-energy tubes. This finding suggests that signal energy CT with a tin-filtered high-voltage tube can provide substantial metal artifact reduction when MAR is applied. However, further research is

 https://doi.org/10.3348/kjr.2020.0548

required on this topic.

Our study had several limitations. First, due to insufficient data resources not all cases could be used for quantitative analysis. Second, our results may have limited validity for other vendors using different dual-energy techniques and MARs because CT scans were acquired using one type of DECT scanner and MAR method. Third, we used only the soft tissue kernel (I40). Soft tissue kernels and sharp kernels have their own pros and cons. Sharp kernels are more suitable to evaluate bone and high-density materials but have more noise, whereas soft tissue kernels are more suitable for soft tissue and bone marrow and have less noise. Thus, considering the study purpose of reduction of metallic artifacts and noise, the soft tissue kernel may not be an inferior choice. Fourth, qualitative image quality was not evaluated separately in soft tissue and bone windows, but only in a single window set of 600/150 HU. In general, soft tissue and bone windows are good to evaluate soft tissue and bone, respectively. However, a window set of 600/150 HU may offer benefits in patients undergoing knee arthroplasty. CT attenuation numbers of the bone become lower in the images with higher kVp. Moreover, most patients undergoing knee arthroplasty are older, and the procedures worsen their osteoporosis. Thus, it is more difficult to evaluate bony abnormalities in CT images with bone windows. In the soft tissue window, the image quality, particularly of the non-iMAR image series, was too poor for assessing the abnormality in the vicinity of the prosthesis. A window range/level of 600/150 HU is a hybrid between that of bone and soft tissue, and may compensate for soft tissue differentiation and low bone density in bone windows and metal artifacts in soft tissue windows to some degree. Fifth, high-density artifact quantification included metallic implants and sometimes cortical bone. Sixth, the detectability of abnormalities was not evaluated. This is because all cases included in this study were routinely examined at follow-up 3 months after knee arthroplasty, and there were no significant abnormalities to evaluate. Lastly, this study was only exploratory. Although we applied Bonferroni adjustment to interpret the statistical significance of the comparisons, some of the statistically significant differences might have turned up by chance due to the presence of a massive number of hypothesis tests. Further confirmatory research studies are needed.

In conclusion, iMAR-applied, linearly blended polychromatic images with low weighting factors ($P_{-0.3i}$ and $P_{0.0i}$) improved image quality compared to iMAR-applied monochromatic images in patients with total knee arthroplasty. If DECT is available, we would recommend obtaining both $P_{-0.3i}$ and $P_{0.0i}$, because $P_{-0.3i}$ substantially decreases metal artifacts and increases visibility of the bone-metal interface, and $P_{0.0i}$ provides a good CNR along with considerable metal artifact reduction.

Conflicts of Interest

The authors have no potential conflicts of interest to disclose.

Author Contributions

Conceptualization: Hye Jung Choo, Dong Wook Kim. Data curation: Hye Jung Choo, Yoo Jin Lee, Sun Joo Lee, Jin Wook Baek, Ji-yeon Han, Young Jin Heo. Formal analysis: Hye Jung Choo, Sun Joo Lee. Investigation: Hye Jung Choo, Sun Joo Lee, Jin Wook Baek. Methodology: Sun Joo Lee, Dong Wook Kim, Yoo Jin Lee. Project administration: Hye Jung Choo. Resources: Ji-yeon Han, Young Jin Heo. Software: Yoo Jin Lee, Ji-yeon Han, Jin Wook Baek. Supervision: Dong Wook Kim. Validation: Ji-yeon Han, Jin Wook Baek, Young Jin Heo. Visualization: Hye Jung Choo, Young Jin Heo, Yoo Jin Lee. Writing—original draft: Hye Jung Choo. Writing—review & editing: all authors.

ORCID iDs

Hye Jung Choo
https://orcid.org/0000-0003-3941-6989
Sun Joo Lee
https://orcid.org/0000-0001-6210-9720
Dong Wook Kim
https://orcid.org/0000-0002-9826-1326
Yoo Jin Lee
https://orcid.org/0000-0003-4701-7339
Jin Wook Baek
https://orcid.org/0000-0003-4632-4951
Ji-yeon Han
https://orcid.org/0000-0003-3780-358X
Young Jin Heo
https://orcid.org/0000-0002-4765-0727

REFERENCES

1. Khodarahmi I, Fishman EK, Fritz J. Dedicated CT and MRI techniques for the evaluation of the postoperative knee. *Semin Musculoskelet Radiol* 2018;22:444-456
2. Katsura M, Sato J, Akahane M, Kunimatsu A, Abe O. Current

https://doi.org/10.3348/kjr.2020.0548

and novel techniques for metal artifact reduction at CT: practical guide for radiologists. *Radiographics* 2018;38:450-461
3. Barrett JF, Keat N. Artifacts in CT: recognition and avoidance. *Radiographics* 2004;24:1679-1691
4. Wellenberg RHH, Hakvoort ET, Slump CH, Boomsma MF, Maas M, Streekstra GJ. Metal artifact reduction techniques in musculoskeletal CT-imaging. *Eur J Radiol* 2018;107:60-69
5. Guggenberger R, Winklhofer S, Osterhoff G, Wanner GA, Fortunati M, Andreisek G, et al. Metallic artefact reduction with monoenergetic dual-energy CT: systematic ex vivo evaluation of posterior spinal fusion implants from various vendors and different spine levels. *Eur Radiol* 2012;22:2357-2364
6. Yoo HJ, Hong SH, Chung BM, Moon SJ, Choi JY, Chae HD, et al. Metal artifact reduction in virtual monoenergetic spectral dual-energy CT of patients with metallic orthopedic implants in the distal radius. *AJR Am J Roentgenol* 2018;211:1083-1091
7. Lewis M, Reid K, Toms AP. Reducing the effects of metal artefact using high keV monoenergetic reconstruction of dual energy CT (DECT) in hip replacements. *Skeletal Radiol* 2013;42:275-282
8. Bolstad K, Flatabø S, Aadnevik D, Dalehaug I, Vetti N. Metal artifact reduction in CT, a phantom study: subjective and objective evaluation of four commercial metal artifact reduction algorithms when used on three different orthopedic metal implants. *Acta Radiol* 2018;59:1110-1118
9. Bongers MN, Schabel C, Thomas C, Raupach R, Notohamiprodjo M, Nikolaou K, et al. Comparison and combination of dual-energy-and iterative-based metal artefact reduction on hip prosthesis and dental implants. *PLoS One* 2015;10:e0143584
10. Khodarahmi I, Haroun RR, Lee M, Fung GSK, Fuld MK, Schon LC, et al. Metal artifact reduction computed tomography of arthroplasty implants: effects of combined modeled iterative reconstruction and dual-energy virtual monoenergetic extrapolation at higher photon energies. *Invest Radiol* 2018;53:728-735
11. Laukamp KR, Zopfs D, Lennartz S, Pennig L, Maintz D, Borggrefe J, et al. Metal artifacts in patients with large dental implants and bridges: combination of metal artifact reduction algorithms and virtual monoenergetic images provides an approach to handle even strongest artifacts. *Eur Radiol* 2019;29:4228-4238
12. Long Z, DeLone DR, Kotsenas AL, Lehman VT, Nagelschneider AA, Michalak GJ, et al. Clinical assessment of metal artifact reduction methods in dual-energy CT examinations of instrumented spines. *AJR Am J Roentgenol* 2019;212:395-401
13. Neuhaus V, Grosse Hokamp N, Zopfs D, Laukamp K, Lennartz S, Abdullayev N, et al. Reducing artifacts from total hip replacements in dual layer detector CT: combination of virtual monoenergetic images and orthopedic metal artifact reduction. *Eur J Radiol* 2019;111:14-20
14. Graser A, Johnson TR, Chandarana H, Macari M. Dual energy CT: preliminary observations and potential clinical applications in the abdomen. *Eur Radiol* 2009;19:13-23
15. Kim KS, Lee JM, Kim SH, Kim KW, Kim SJ, Cho SH, et al. Image fusion in dual energy computed tomography for detection of hypervascular liver hepatocellular carcinoma: phantom and preliminary studies. *Invest Radiol* 2010;45:149-157
16. Behrendt FF, Schmidt B, Plumhans C, Keil S, Woodruff SG, Ackermann D, et al. Image fusion in dual energy computed tomography: effect on contrast enhancement, signal-to-noise ratio and image quality in computed tomography angiography. *Invest Radiol* 2009;44:1-6
17. Landis JR, Koch GG. The measurement of observer agreement for categorical data. *Biometrics* 1977;33:159-174
18. Primak AN, Ramirez Giraldo JC, Liu X, Yu L, McCollough CH. Improved dual-energy material discrimination for dual-source CT by means of additional spectral filtration. *Med Phys* 2009;36:1359-1369
19. Zhou W, Bartlett DJ, Diehn FE, Glazebrook KN, Kotsenas AL, Carter RE, et al. Reduction of metal artifacts and improvement in dose efficiency using photon-counting detector computed tomography and tin filtration. *Invest Radiol* 2019;54:204-211

 https://doi.org/10.3348/kjr.2020.0548